Available online at www.sciencedirect.com
ScienceDirect
Soils and Foundations 63 (2023) 101325
www.elsevier.com/locate/sandf

Technical Paper

Modified ultimate bearing capacity formula of strip footing on sandy soils considering strength non-linearity depending on stress level

Tahir Iqbal [a,*], Satoru Ohtsuka [b], Koichi Isobe [c], Yutaka Fukumoto [b], Kazuhiro Kaneda [d]

[a] *Department of Energy and Environmental Engineering, Nagaoka University of Technology, 1603-1 Kamitomioka, Nagaoka, Niigata 940-2188, Japan*
[b] *Department of Civil and Environmental Engineering, Nagaoka University of Technology, 1603-1 Kamitomioka, Nagaoka, Niigata 940-2188, Japan*
[c] *Division of Field Engineering for Environment, Hokkaido University, 13 Kita, 8 Nishi, Kita-ku, Sapporo, Hokkaido 060-8628, Japan*
[d] *Department of Civil Engineering, Chiba Institute of Technology, 2-17-1 Tsudanuma, Narashino, Chiba 275-0016, Japan*

Received 7 December 2022; received in revised form 21 April 2023; accepted 7 May 2023

Abstract

Most of the contemporary ultimate bearing capacity (UBC) formulas assume a linear yield function in shear stress-normal stress space. However, experimental investigations have corroborated the non-linearity in the failure envelopes of sandy soils. This study focused on the assessment of the stress level effect on the UBC of surface strip footings ascribed to the soil unit weight (γ), footing size (B), and uniform surcharge load (q). The rigid plastic finite element method (RPFEM) was employed for the analysis. The analysis method was validated against the centrifuge test results from the published references in the case of various sandy soils with different relative densities. The RPFEM, using the mean confining stress dependence property of Toyoura sand, is utilized in non-linear finite element analysis of model sandy soil. The normalized ground failure domains in the case of the non-linear shear strength model are gleaned smaller than those in the case of the linear shear strength one. The numerical results are compared with the guidelines of the Architectural Institute of Japan (AIJ) and the Japan Road Association (JRA). The modification coefficients are ascertained for the frictional bearing capacity factor (N_γ) and surcharge bearing capacity factor (N_q), and a modified UBC formula is proposed. The performance of the proposed UBC formula is examined against the analysis results and various prevailing UBC guidelines.

Keywords: Ultimate bearing capacity; Strip footing; Footing size effect; Non-linear shear strength; Sandy soils; Rigid plastic finite element method

1. Introduction

It is well recognized that the footing size has a substantial effect on the ultimate bearing capacity (UBC) of sandy soils, thereby rendering significant uncertainty when choosing the appropriate UBC formula accounting for the size effect phenomenon. It is relevant to mention that, as the footing size increases, the confining stresses in the soil increase and the dilatancy decreases. This results in a reduced peak friction angle, and hence, causes a significant drop in the UBC results. The size of the footing affects the UBC through the confining stress dependency of shear strength parameter ϕ (Ueno et al., 1998; Zhu et al., 2001).

In view of such bearing capacity problems, it is pertinent to note that the mean effective stress in the failure domain is a function of both soil unit weight γ and footing size B through its dependency on the limit bearing pressure. Therefore, both the footing size and the soil unit weight are of paramount importance when estimating the confining stress dependency of the shear strength parameters.

* Corresponding author.
E-mail addresses: engr.tahiriqbalgujjar@gmail.com, s195075@stn.nagaokaut.ac.jp (T. Iqbal), ohtsuka@vos.nagaokaut.ac.jp (S. Ohtsuka), kisobe@eng.hokudai.ac.jp (K. Isobe), yfukumoto@vos.nagaokaut.ac.jp (Y. Fukumoto), kazuhiro.kaneda@p.chibakoudai.jp (K. Kaneda).

https://doi.org/10.1016/j.sandf.2023.101325
0038-0806/

Some experimental studies have used the term γB to discuss the size effect of footings on the UBC (De Beer, 1965; Ueno et al., 1998). Furthermore, footings are often subjected to heavy overburdens induced by adjoining landfills, which may lead to incremental confining pressure in the bearing stratum and result in a reduced peak friction angle.

In the purview of the preceding discussion, a confining stress-dependent simplified UBC formula, accounting for the effect of the aforementioned factors, is still lacking. Therefore, the aim of this research was to study the extensive UBC analysis of surface strip footings in order to reckon the influence of the size effect phenomenon on the UBC. The rigid plastic finite element method (RPFEM) program code was employed for the UBC analysis in the case of sandy soils considering centric vertical and uniform surcharge loads.

Nguyen et al. (2016) used the non-linear shear strength property of Toyoura sand to estimate the size effect of footings on the UBC. However, the present research employs the mean confining stress property of Toyoura sand for the UBC analysis in the case of a model sandy soil. In addition, the scope of this study is extended to widely investigate the confining stress dependency of the UBC as a function of soil unit weight γ, footing size B, and uniform surcharge load q. The challenge of a UBC assessment using a stability analysis is to consider the effect of the progressive failure on the UBC due to the shear property of the strain softening of dense sandy soils. However, many researchers (e.g., Hettler and Gudehus, 1988; Nguyen et al., 2016) have clarified successful assessments of the UBC of strip footings by employing the peak shear strength parameters of sandy soils in triaxial compression tests.

The core of the present study comprises three sections. Initially, the shear strength properties of various sandy soils are investigated, and the performance of the RPFEM is evaluated in terms of its ability to compute the UBC in comparison to experimental studies using centrifuge model tests. In the subsequent section, a UBC analysis of a model sandy soil is conducted based on the mean shear strength property of Toyoura sand. In addition, the results elicited from the linear and non-linear shear strength criteria are compared to elucidate the features of the non-linear shear strength analysis technique and its advantages over the Drucker-Prager (linear) model. Moreover, the ground failure domains are thoroughly examined to understand the effect of the footing size on the strain rate distribution and the size of the failure domain in the cases of total and effective stress analysis conditions. Finally, a new UBC formula is proposed to account for the stress dependency through modification coefficients, and its performance is assessed in comparison with the RPFEM analysis and various existing UBC guidelines.

2. Literature review of some prevailing ultimate bearing capacity formulas

Some prominent UBC formulas for strip footings on uniform sandy soils under centric vertical and uniform surcharge loads are arranged in Table 1. Classically, the UBC of strip footings on uniform sandy soil deposits is expressed as follows:

$$q_u = \frac{1}{2}\gamma B N_\gamma + qN_q \tag{1}$$

In Eq. (1), q_u represents the ultimate bearing capacity, and N_γ and N_q symbolize the bearing capacity factors due to the self-weight and uniform surcharge load, respectively, depending solely on the internal friction angle of the soil, ϕ. Furthermore, γ denotes the unit weight of the soil underneath the footing, B accounts for the footing size, and q is the uniform surcharge load. Meyerhof (1963) endorsed the closed-form expression for the bearing capacity factor, N_q, as given in Table 1, which was initially proposed by Prandtl (1921) and Reissner (1924) and later corroborated by various other researchers (e.g., Vesić, 1973, 1975).

A completely accurate closed-form analytical solution has not yet been determined for N_γ, despite numerous attempts in various research studies. This is partly owing to the size effect and difficulty associated with the selection of the appropriate friction angle while comparing the theoretical UBC with that of the test results (Hijaj et al., 2005). Furthermore, studies have highlighted the state dependency of the internal friction angle, significantly influenced by the stress level and soil relative density (e.g., Salgado et al., 2000). The N_γ relationship proposed by Meyerhof (1963) is depicted in Table 1; it is one of the most widely used expressions for N_γ (Poor et al., 2015).

The UBC formula recommended in the engineering manual for the bearing capacity of soils (EM 1110–1–1905) by the U.S. Army Corps of Engineers (USACE, 1992) considers the effect of the stress level on the UBC through the modification coefficient in the frictional term of the UBC formula. According to the USACE engineering manual, the choice of bearing capacity factors depends on the type of model selected, namely, Terzaghi, Meyerhof, Hansen, or Vesić. In the case of shallow foundations, both the Soils and Foundations reference manual of the U.S. Federal Highway Administration (FHWA, 2006) and the bridge design specifications of the American Association of State Highway and Transportation Officials (AASHTO, 2020) recommend using the bearing capacity factors, which is the same as the recommendation given in Vesić (1973, 1975). Therefore, the bearing capacity factors of Vesić (1973, 1975) are used for UBC estimation in the case of the USACE UBC formula in this study.

The simplified UBC relationship derived from the plasticity theory and the experimental results, as proposed in the European standard for geotechnical design, i.e., Eurocode 7 (EN 1997–1:2004), is practically the same as that given in Eq. (1) for strip footings on sandy soils. The relationships for the bearing capacity factors are presented in Table 1.

The UBC formulas being used in Japan are those developed by the Architectural Institute of Japan (AIJ, 1988,

Table 1
Comparison of various simplified UBC formulas for strip footings on sandy soils in terms of stress effect modification coefficients.

Author/guideline	Formula	Bearing capacity factors		Stress effect modification coefficients	
		N_γ	N_q	η_γ	η_q
Meyerhof (1963)	$q_u = \frac{1}{2}\gamma B N_\gamma + q N_q$	$(N_q - 1)\tan(1.4\phi)$	$\exp(\pi\tan\phi)\tan^2\left(45^o + \frac{\phi}{2}\right)$	No	No
U.S. Army Corps of Engineers (USACE, 1992)	$q_u = \frac{1}{2}\gamma B \eta_\gamma N_\gamma + q N_q$	$2(N_q + 1)\tan\phi$	$\exp(\pi\tan\phi)\tan^2\left(45^o + \frac{\phi}{2}\right)$	$1 - 0.25\log\left(\frac{B}{B_o}\right)$ $B_o = 2\ m$	No
Eurocode 7 (EN 1997–1:2004)	$q_u = \frac{1}{2}\gamma B N_\gamma + q N_q$	$2(N_q - 1)\tan\phi$	$\exp(\pi\tan\phi)\tan^2\left(45^o + \frac{\phi}{2}\right)$	No	No
Japan Road Association (JRA, 2017)	$q_u = \frac{1}{2}\gamma B \eta_\gamma N_\gamma + q \eta_q N_q$	Graphic curves	Graphic curves	$(B)^{\frac{-1}{3}}$	$(q^*)^{\frac{-1}{3}}$ $q^* = \frac{q}{q_o}(1 \leq q^* \leq 10)$ $q_o = 10$ kPa
Architectural Institute of Japan (AIJ, 1988, 2001, 2019)	$q_u = \frac{1}{2}\gamma B \eta_\gamma N_\gamma + q N_q$	$(N_q - 1)\tan(1.4\phi)$	$\exp(\pi\tan\phi)\tan^2\left(45^o + \frac{\phi}{2}\right)$	$\left(\frac{B}{B_o}\right)^{\frac{-1}{3}}$ $B_o = 1\ m$	No

Notes: B_o = Reference footing width, q_o = Reference surcharge load.

2001, 2019) and the Japan Road Association (JRA) in the Road bridge specifications (2017). The AIJ guidelines consider the stress level effect through the modification coefficient only in the frictional term of the UBC formula. However, the JRA guidelines have introduced stress effect modification coefficients in both frictional and surcharge terms of the UBC formula. The bearing capacity factors in the AIJ guidelines correspond to those proposed by Meyerhof (1963). In the JRA guidelines, however, graphical curves are used for the bearing capacity factors. They are practically the same as those used in Meyerhof (1963).

The limitations of the conventional UBC formulas, in terms of the influence of various factors when estimating the confining stress dependency of the UBC and the inconsistencies amongst the different guidelines for the modification coefficients, need to be thoroughly investigated and thereby uphold the importance of the present research.

3. Constitutive equations for finite element analysis of rigid footing

In this research, the UBC analysis was carried out using the in-house RPFEM program code developed by the authors (Hoshina et al., 2011; Nguyen et al., 2016). The RPFEM stems from the upper bound theorem of plasticity which, in fact, applies the upper bound on the true collapse load to be determined. The rigid plastic constitutive equation was initially developed for frictional materials by Tamura et al. (1987). Moreover, the applicability of the RPFEM was thoroughly examined and endorsed previously in the purview of geotechnical stability problems (Asaoka and Ohtsuka, 1986, 1987; Asaoka et al., 1990; Nguyen et al., 2016).

In this study, the UBC analysis is performed using the RPFEM based on the linear (i.e., Drucker-Prager (DP)) and non-linear (NL) yield functions. The non-linear rigid plastic constitutive equation, introduced by Nguyen et al. (2016) for sandy soils, was employed. It can accurately account for the various material properties and their mutual dependence, such as the confining stresses and angles of internal friction. Details of the non-linear yield function and rigid plastic constitutive equation are provided in this section, while those of the Drucker-Prager yield criterion can be found in the articles published by the authors (Pham et al., 2019a, 2019b, 2020; Pham and Ohtsuka, 2021; Pham et al., 2022). Nguyen et al. (2016) refined the RPFEM to account for the effect of particle breakage on the stress-dependent shear strength property of sandy soils by applying a higher order yield function, as follows:

$$f(\boldsymbol{\sigma}) = aI_1 + (J_2)^n - b = 0 \tag{2}$$

Here, a and b are the soil parameters corresponding to internal friction angle ϕ and cohesion c, respectively, retrieved through the experimental data from strength tests on a given soil. Furthermore, n depicts the non-linearity of the failure envelope in relation to the first stress invariant, I_1, and the second invariant of deviator stress, J_2. The non-linear yield function (Eq. (2)) is used under the plane strain condition by considering the associated flow rule. The non-linear yield function (Eq. (2)) has been successfully applied to bearing capacity problems of footings and piles, using the rigid plastic constitutive equation, in the case of ϕ and c-ϕ soils, and has been shown to adequately demonstrate the stress dependency of the soil strength in published research articles by the authors (Hoshina et al., 2011; Nguyen et al., 2016; Tamboura et al., 2022). Based on the associated flow rule, strain rate $\dot{\boldsymbol{\varepsilon}}$ is obtained for the non-linear yield function presented in Eq. (2) as follows:

$$\dot{\boldsymbol{\varepsilon}} = \lambda\frac{\partial f(\boldsymbol{\sigma})}{\partial \boldsymbol{\sigma}} = \lambda\frac{\partial}{\partial \boldsymbol{\sigma}}\left(aI_1 + (J_2)^n - b\right) = \lambda\left(a\boldsymbol{I} + nJ_2^{n-1}\boldsymbol{s}\right) \tag{3}$$

In Eq. (3), λ is the plastic multiplier, and $\boldsymbol{I}$ and $\boldsymbol{s}$ indicate the unit and deviatoric stress tensors, respectively. The correlation for the norm of the strain rate is given as Eq. (4).

$$\dot{e} = \sqrt{\dot{\boldsymbol{\varepsilon}}:\dot{\boldsymbol{\varepsilon}}} = \lambda\sqrt{3a^2 + n^2J_2^{2n-2}2J_2} = \lambda\sqrt{3a^2 + 2n^2J_2^{2n-1}} \tag{4}$$

The relationship for plastic multiplier λ is finally derived as follows:

$$\lambda = \frac{\dot{e}}{\sqrt{3a^2 + 2n^2(b - aI_1)^{2-1/n}}} \tag{5}$$

The volumetric strain rate is expressed as follows:

$$\begin{aligned} \dot{\varepsilon}_v &= \mathrm{tr}\dot{\boldsymbol{\varepsilon}} = \mathrm{tr}\left(\lambda\left(a\boldsymbol{I} + nJ_2^{n-1}\boldsymbol{s}\right)\right) = 3a\lambda \\ &= \frac{3a}{\sqrt{3a^2 + 2n^2(b - aI_1)^{2-1/n}}}\dot{e} \end{aligned} \tag{6}$$

where $\dot{\varepsilon}_v$ and $\dot{e}$ depict the volumetric strain rate and the norm of the strain rate, respectively. The first stress invariant is ascertained from Eqs. (2) to (6) as the following relationship:

$$\boldsymbol{I}_1 = \frac{b}{a} - \frac{1}{a}\left\{\frac{1}{2n^2}\left[\left(3a\frac{\dot{e}}{\dot{\varepsilon}_v}\right)^2 - 3a^2\right]\right\}^{\frac{n}{2n-1}} \tag{7}$$

The deviatoric stress is identified from Eq. (3) as follows:

$$\boldsymbol{s} = \frac{1}{n}\left(3a\frac{\dot{\boldsymbol{\varepsilon}}}{\dot{\varepsilon}_v} - a\boldsymbol{I}\right)\left\{\frac{1}{2n^2}\left[\left(3a\frac{\dot{e}}{\dot{\varepsilon}_v}\right)^2 - 3a^2\right]\right\}^{\frac{1-n}{2n-1}} \tag{8}$$

The non-linear rigid plastic constitutive equation for confining pressure is finally obtained through Eqs. (7) and (8) as follows (Nguyen et al., 2016; Tamboura et al., 2022):

$$\begin{aligned} \boldsymbol{\sigma} = &\frac{3a}{n}\left\{\frac{1}{2n^2}\left[\left(3a\frac{\dot{e}}{\dot{\varepsilon}_v}\right)^2 - 3a^2\right]\right\}^{\frac{1-n}{2n-1}}\frac{\dot{\boldsymbol{\varepsilon}}}{\dot{\varepsilon}_v} \\ &+ \left(\frac{b}{3a} - \frac{1}{3a}\left[\frac{1}{2n^2}\left(3a\frac{\dot{e}}{\dot{\varepsilon}_v}\right)^2 - 3a^2\right]^{\frac{n}{2n-1}}\right. \\ &\left. - \frac{a}{n}\left[\frac{1}{2n^2}\left(3a\frac{\dot{e}}{\dot{\varepsilon}_v}\right)^2 - 3a^2\right]^{\frac{1-n}{2n-1}}\right)\boldsymbol{I} \end{aligned} \tag{9}$$

The non-linear yield function (Eq. (2)) corresponds to the Drucker-Prager yield function in the case of $n = 0.5$. However, it is noted that the rigid plastic constitutive equation (Eq. (9)) is not applicable in the above case. It is pertinent to point out that, in the case of the rigid plastic constitutive equation for the Drucker-Prager yield criterion, the stress is split into two components, one of which is uniquely determined for the strain rate, and the other of which is indeterminate and determined by solving the equilibrium equation in consideration of the constraint condition on the strain rate, such as the dilatancy property for the Drucker-Prager yield function (Nguyen et al., 2016; Tamboura et al., 2022). On the contrary, in the case of the non-linear yield function, the stress is uniquely defined for the plastic strain rate.

4. Discussion on non-linear shear strength property of sandy soils

4.1. Shear strength property of various sandy soils

This research primarily focuses on the stress-dependent shear strength property of Toyoura sand, which is one of the most commonly used sandy soils for research in Japan. Furthermore, the shear strength property of other sandy soils, i.e., silica and Silver Leighton Buzzard (S.L.B) sands, is also investigated to grasp the general trend in the stress dependency of sandy soils. The index properties of various sandy soils examined in this study are arranged in Table 2.

In the present study, the confining stress dependency of the frictional material, i.e., Toyoura sand, is modeled based on the strength tests of Tatsuoka et al. (1986), since the compression tests were conducted under low to high confining pressures (4.9 kPa to 392 kPa) with very loose to very dense particle distributions. For a given relative density, the experimental results indicate a decreasing trend in the internal friction angle with increasing confining pressure. In the first instance, the experimental results are arranged for various relative densities (Fig. 1) to grasp the change in internal friction angle corresponding to the various stress levels through the first stress invariant I_1 at the critical state. The negative values for I_1 refer to the compression stress. Through case studies, the experimental data are extrapolated to estimate the y-intercept, i.e., initial internal friction angle (ϕ_0) against each relative density (D_r), as shown by the dashed lines in Fig. 1. Such extrapolation is useful for firstly establishing a normalized relationship for the internal friction angle at various stress levels corresponding to the initial state and then later comparing the ultimate bearing capacity of the model sandy soil with conventional UBC formulas for a given initial internal friction angle. The relationship between the normalized internal friction angle and the first stress invariant is established in Fig. 2. Regardless of the variation in D_r, the relationship between the normalized internal friction angle and the first stress invariant reveals the common property. As the various relative densities represent nearly similar material responses under stress, it is meaningful to develop a simplified relationship based on the mean property of Toyoura sand against various confining stress levels. The mean trend line is plotted in Fig. 2 using the least squares method. In Fig. 2, the reference value for the mean stress for the normalization of the internal friction angle is set to zero. However, the normalized internal friction angle was verified against the normalized mean stress by Nguyen et al. (2016) and showed a coincident trend, even when the reference values for internal friction angle ϕ_0 and first stress invariant I_{10} were purposely set at different values, which suggests the wide applicability of Fig. 2.

The effect of the confining pressure on the internal friction angle is witnessed in the case of most sands, gravels, and ballast, being a general characteristic (Hettler and Gudehus, 1988). Therefore, it is relevant to survey the stress dependency of the internal friction angle in the case of various sandy soils. Based on the strength tests of Zhu et al. (2001) and Yoshida et al. (1995, 1997), respectively, the stress-dependent shear strength property of silica and S.L.B sands is investigated in comparison with that of the Toyoura sand in this study. The normalized internal friction angle of various sandy soils decreases with an

Table 2
Index properties of various sandy soils.

Soil (Origin)	Mean grain size d_{50} (mm)	Uniformity coefficient C_u	Specific gravity G_s	Maximum void ratio e_{max}	Minimum void ratio e_{min}	Grain shape	Minerology	Citation
Silica sand (Canada)	0.22	1.69	2.66	1.060	0.650	Angular to subrounded	95% quartz	Zhu et al. (2001)
S.L.B sand (UK)	0.62	1.11	2.66	0.790	0.490	Subrounded	98% quartz	Yoshida et al. (1995, 1997)
Toyoura sand (Japan)	0.16	1.46	2.64	0.977	0.605	Angular to sub-angular	90% quartz	Yoshimi et al. (1978), Tatsuoka et al. (1986a)

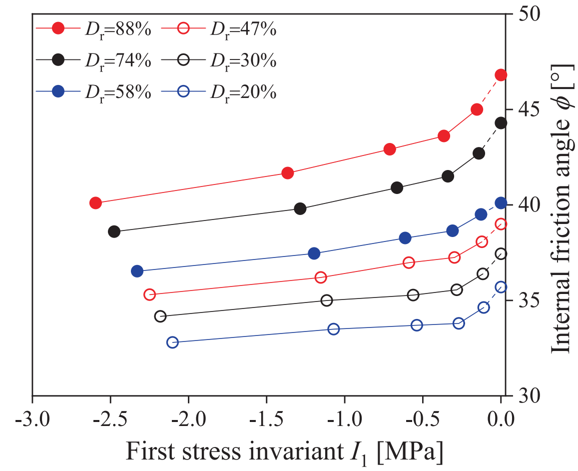

Fig. 1. Relationship between internal friction angle and first stress invariant for Toyoura sand (after Tatsuoka et al. (1986)).

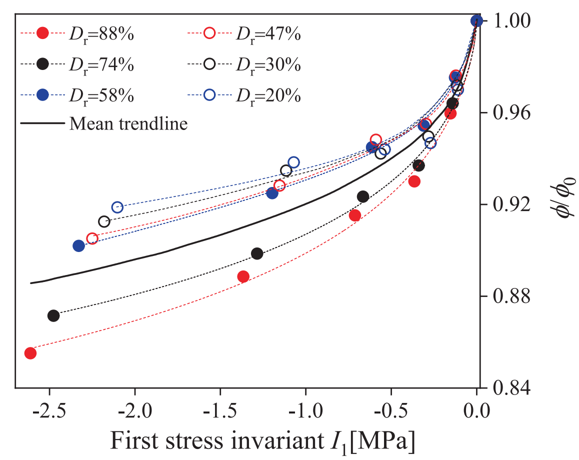

Fig. 2. Normalized relationship between ϕ/ϕ_0 and I_1 for Toyoura sand.

increase in the stress level (Fig. 3). The normalized relationships for silica and S.L.B sands are closely related to those of the Toyoura sand, indicating the typical behavior of

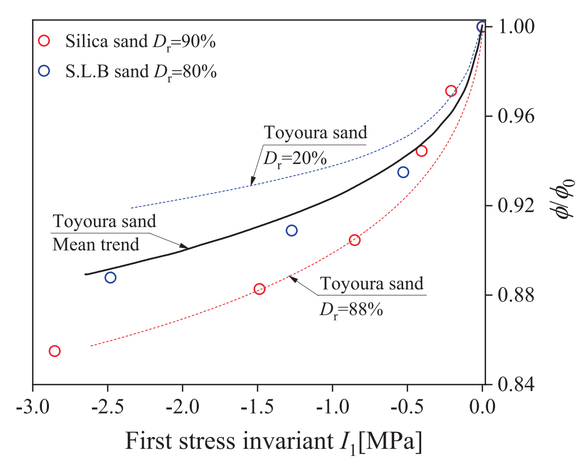

Fig. 3. Comparison of normalized relationship between ϕ/ϕ_0 and I_1 for various sandy soils.

sandy soils with incremental stress (Fig. 3). The normalization between ϕ and I_1 always holds irrespective of the reference value of the confining pressure in standardizing ϕ (Nguyen et al., 2016). Hettler and Gudehus (1988) investigated the influence of the confining pressure on the shear strength property in the case of three different sandy soils, namely, Darmstadt sand, Degebo sand, and Eastern Scheldt sand, through compression tests performed with an improved apparatus. Their experimental study concluded that the parameter which determines the effect of the pressure level on ϕ remained nearly the same in the case of different sands and different relative densities. Although the sandy soils investigated in this study are different from those of Hettler and Gudehus (1988), they indicate the same trend against incremental stress, indicating the general property of sandy soils. The general equation for the mean trendline in Figs. 2 and 3 can be expressed as follows:

$$\frac{\phi}{\phi_0} = \frac{1+\delta I_1}{1+\zeta I_1 + \psi I_1^2} \tag{10}$$

Here,δ depicts the linear coefficient of the numerator, whereas ζ and ψ denote the linear and binomial coefficients of the denominator, enumerated as -1.915 (1/Pa), -2.145 (1/Pa), and 2.105×10^{-5}(1/Pa^2), respectively.

4.2. Validation of simulation method

In this section, the simulation method is corroborated against the centrifuge experimental results in the case of three different sandy soils, namely, silica sand, S.L.B sand, and Toyoura sand, having different relative densities. The RPFEM(NL) is used for the UBC analysis of surface strip footings using soil properties identical to those of the centrifuge experiments in the case of each soil. The soil index properties (Table 2) and the stress-dependent shear strength relationships (Figs. 2 and 3) discussed in the previous section are used for the UBC analysis corresponding to each target soil and relative density. Non-linear parameters, a, b, and n are set in this study to correspond to each soil with a given relative density for the UBC analysis against the centrifuge tests, as can be observed in Fig. 4. The normalized relationships between ϕ/ϕ_0 and I_1 are established in Figs. 2 and 3 for each sandy soil and given relative density. Therefore, the shear strength parameters of the non-linear shear strength are set based on the established trendline relationship (Figs. 2 and 3) for the target soil and relative density, with the same initial internal friction angle as that of the target sand at a given relative density.

Since centrifuge experiments were conducted up to a strip footing width of 4 m, the UBC analysis discussed in this section was conducted up to the same footing size as that which corresponds to the experimental results depicted in Fig. 4. For strip footings on Toyoura sand, the analysis results are compared with the findings of Okahara et al. (1988) in the case of three different relative densities

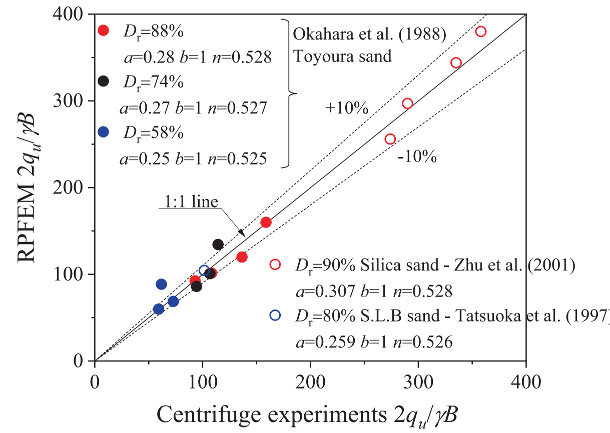

Fig. 4. Validation of analysis method for various sandy soils in cases of B up to 4 m.

(D_r = 58%, 74%, and 88%). In the case of S.L.B sand ($D_r = 80\%$) and silica sand ($D_r = 90\%$), the analysis results are compared with the experimental studies of Tatsuoka et al. (1997) and Zhu et al. (2001), respectively, by employing the shear strength property of each target soil. There is a good agreement between the analysis results of the present study and the centrifuge experimental findings, as can be observed in Fig. 4. This indicates that the RPFEM using the non-linear shear strength property of sandy soils can accurately estimate the effect of the footing size on the UBC in the case of various sandy soils ranging from lower to higher relative densities.

5. Ultimate bearing capacity analysis for model sandy soil

5.1. Shear strength property of model sandy soil

In this section the shear strength property of the model sandy soil is discussed. It is useful to consider the model sandy soil for comparing the UBC estimated through the RPFEM and various UBC formulas from literature for a given initial internal friction angle. According to Peck et al. (1974), the internal friction angles of loose to dense sandy soils normally fall in the range of 28.5° to 41°. Therefore, a reasonably wide range of friction angles, i.e., $\phi_0 = 30^\circ$-40°, is considered for the model sandy soil, as soils falling in this range are often encountered in practice. Established for the mean property of Toyoura sand (Figs. 2 and 3), the non-linear shear strength parameters can easily be set for model sandy soil with a given initial internal friction angle as normally retrieved through triaxial compression tests. The model sandy soil is defined by the shear strength property, which follows the mean trendline (Eq. (10)) of the shear strength for Toyoura sand. Therefore, the shear strength parameters of the non-linear shear strength are set based on the mean trendline (Eq. (10)) through the triaxial compression condition, and initial internal angle ϕ_0 is set as that of the target model sandy soil.

The initial friction angle is set to correspond to the reference value in the first stress invariant, i.e., $I_1 = 0$ MPa, and the model parameters are set through the non-linear yield function (Eq. (2)) based on the relationship between I_1 and $\sqrt{J_2}$ of the target model sandy soil, as shown in Fig. 5. The non-linear parameters, a, b, and n, are depicted in Table 3 for bearing capacity analyses in the case of the model sandy soil. Parameter n expresses the non-linearity of the shear strength against the stress level, and a corresponds to the initial internal friction angle ϕ_0 of the target model sand. Therefore, n is uniquely set by the mean trend-line property of the shear strength in Eq. (10), and a is determined by fitting the relationship of I_1 and $\sqrt{J_2}$ for the target internal friction angle ϕ_0 drawn by considering Eq. (10) and the stress condition of the triaxial compression test, as shown in Fig. 5. A marginal value for the cohesion parameter ($b = 1$ kPa) is used in the analysis to stabilize the computations. However, its overall effect on the bearing capacity results is minimal. As the general property of Toyoura sand against the variation in stress levels remains similar for various densities, a constant parameter n is set for the normalized mean relationship in Fig. 2 for the purpose of simplifying the modeling.

5.2. Ultimate bearing capacity analysis using Drucker-Prager and non-linear shear strength

This section focuses on a stability analysis of strip footings on a model sandy soil under the plane strain condition using the RPFEM Drucker-Prager (DP) and RPFEM non-linear (NL). The material shear strength parameters incorporated in the RPFEM(DP) analysis procedure are identical to those gleaned from conventional triaxial compression tests, while in the case of the RPFEM(NL), the parameters set in Table 3 are employed. The UBC analysis is conducted for a wide range of footing sizes (1 m to 10 m) and material shear strength parameters to properly ascertain the efficacy of the employed technique. The material strength characteristics of the footing are set up in such

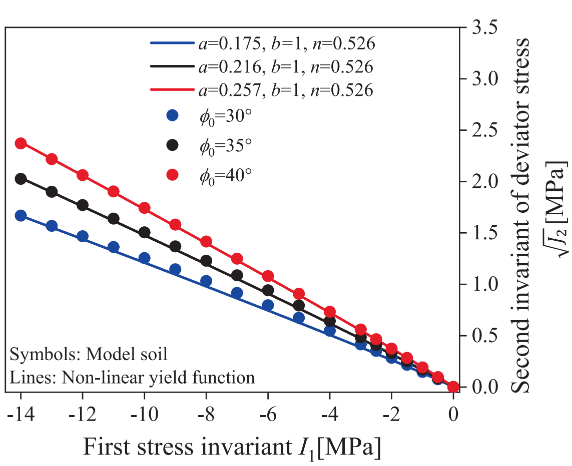

Fig. 5. Relationship between I_1 and $\sqrt{J_2}$ for model sandy soil.

Table 3
Material shear strength parameters for analyses in case of model sandy soil.

ϕ_0	a	b (kPa)	n
30°	0.175	1	0.526
35°	0.216		
40°	0.257		

a manner as to have a completely rigid mass, while the boundary conditions are set to be wide enough so that the rigidity will not have any direct effect on the soil failure domain.

The analysis results through the RPFEM(DP) and RPFEM(NL) are plotted along with those from the Meyerhof, AIJ, and JRA bearing capacity formulas in Fig. 6 for the centric vertical loading scenario in the absence of surcharge loading in the case of $\gamma = 18$ kN/m^3. It is pertinent to mention that both AIJ and JRA guidelines propound the same size effect modification in N_γ in the absence of surcharge loading. The RPFEM (DP), being the linear shear strength model, indicates good concurrence with the Meyerhof UBC formula (Fig. 6). It corroborates that the boundary conditions, mesh size, and loading arrangements considered for the analyses are suitable to precisely compute the ultimate bearing capacity for the various cases examined in this research study.

The marked difference in the results between the RPFEM(DP) and RPFEM(NL) is quite noticeable and can be attributed to the size effect of the footing on the UBC through the confining stress dependency of the shear strength parameters. This is primarily because large footings lead to high stress levels in the soils underneath them, resulting in a reduced peak friction angle. Apropos, such an effect of the stress level on the UBC has been pointed out in numerous experimental studies (De Beer, 1965; Clark, 1998; Zhu et al., 2001) as well as numerical studies (Nguyen et al., 2016). Since the size effect of footings is

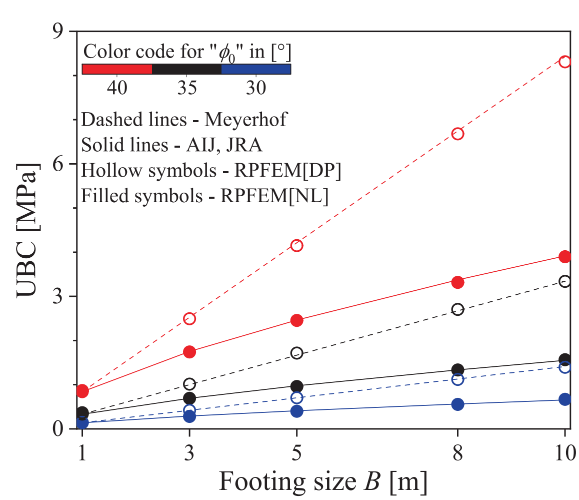

Fig. 6. Comparison of ultimate bearing capacity results in case of $\gamma = 18$ kN/m^3.

an evolving subject, the exact reasons behind this phenomenon have not yet been fully clarified. For instance, Steenfelt (1977) ascribed the size effect to the influence from the ratio of the grain size to the footing width, whilst Hettler and Gudehus (1988) attributed it to the effect of the pressure level on ϕ. Several studies in the recent past have attributed this phenomenon to the stress level effect on the internal friction angle. In this study, therefore, the non-linearity in the shear strength, being a common characteristic of sandy soils, is considered a useful property to better understand this phenomenon and to ascertain its contributing factors.

The RPFEM(NL) analysis results are in good agreement with the AIJ and JRA bearing capacity formulas for a wide range of shear strength in the case of $\gamma = 18$ kN/m^3 under centric vertical load only (Fig. 6). This indicates the effectiveness of the non-linear rigid plastic constitutive equation in estimating the effect of the confining pressure on the shear strength property of the model sandy soil. Nguyen et al. (2016) also evinced the consistency in the bearing capacity analysis results between RPFEM(NL) and AIJ. It is relevant to mention here that, for an increase in footing size from 1 m to 10 m, in the cases of $\phi_0 = 30°$, 35°, and 40°, the RPFEM(NL) leads to a nearly 53% decrease in the UBC results as compared to the RPFEM (DP), as can be observed in Fig. 6. It is germane to delineate that Zhu et al. (2001) reported a 55% reduction in bearing capacity factor N_γ for a 10-fold increase in footing size based on centrifuge experiments using silica sand. Similarly, the experimental investigations of Clark (1998) concluded that bearing capacity factor N_γ generally decreases by nearly 50% for each log cycle increase in footing size. The RPFEM(NL), using the confining stress dependency of Toyoura sand, can accurately simulate the effect of the footing size. However, it is extremely important to carry out a stability analysis for an extensive range of soil unit weights γ to determine its effect on the confining stresses and size of the bearing area. This is primarily because various characteristics are encountered in the practical situation of soils. Furthermore, there are often geographical conditions involving frequent changes in the water table which also ultimately affect the strength characteristics of the underlying soil.

The typical finite element mesh and boundary conditions employed in the stability analysis are manifested in Fig. 7 in the case of $B = 10$ m. However, the extents of the horizontal and vertical boundaries are set so as not to affect the collapse mechanism. Only one half of the geometry is modeled for the stability analysis considering the symmetry of the problem along the centerline. In this typical case, the total numbers of elements and nodes constituting the soil geometry are 2800 and 2911, respectively. A relatively finer mesh is created in the vicinity of the higher stress region for the purpose of accurately simulating the footing-soil failure mechanism at peak loads. The domain of the failure zone is expressed through the contoured distribution of the norm of strain rate $\dot{e}$ in the range of $\dot{e}_{min}$ to $\dot{e}_{max}$. The relative distribution and magnitude of $\dot{e}$ govern the magnitude of the UBC, and the typical failure mode is observed as general shear failure.

5.3. Discussion on total and effective stress analysis conditions

Pragmatically, the water table below the footing is subject to change over time. Moreover, soil layers having distinct strength characteristics are often encountered in the ground strata. Additionally, the deformation in the soil failure zone is necessarily a function of the effective stresses rather than the total stresses. Therefore, a UBC analysis, in terms of the footing size effect and in consideration of the variation in soil unit weight γ, is necessary to accurately perceive the confining stress dependency of the shear strength parameters. In this section, the analysis is performed for the model sandy soil under previous geometrical and boundary conditions (Fig. 7) by considering the effective unit weight of the soil, 8 kN/m^3 (buoyant unit weight), under the scenario of the water table at the ground surface. The bearing capacity analysis results are plotted in Fig. 8.

The results given in Fig. 8 indicate the significant difference in the UBC between the RPFEM(NL) and the AIJ and JRA formulas in the case of an effective stress analysis. This phenomenon can be easily understood by visualizing the confining stress property of sandy soils. This is mainly because the stress level decreases with the decrease in γ; and consequently, the shear strength and UBC increase. Loukidis et al. (2011) also highlighted this effect of soil unit weight γ on the stress level in the soil and concluded that N_γ decreases with the increase in γB and vice versa. Moreover, eminent experimental studies have also considered the soil unit weight, in addition to the footing size, while discussing the stress level effect (De Beer, 1965; Zhu et al., 2001). However, such an effect of soil unit weight γ is not explicitly considered in the size effect modification coefficients proposed by the AIJ and JRA formulas. The effect of the footing size and soil unit weight on the normalized failure domains (D/B and L/B) has also been investigated, as shown in Table 4. "D" indicates the depth of the failure zone from the ground surface, while "L" indicates the horizontal stretch of the failure zone from the centerline, as shown in Fig. 7.

It is noted that the failure zone becomes larger when the internal friction angle is increased. In the case of the non-linear shear strength model, the internal friction angle decreases with an increase in the footing size. Therefore, the peak friction angle differs in accordance with the first stress invariant; hence, the equivalent plastic strain rate is correspondingly distributed in the failure zone. Despite the material constant being the same, the size of the failure zone is smaller in the case of the non-linear shear strength model as compared to that of the linear shear strength model. In the case of the effective stress condition, the non-linear analysis renders the larger failure zone in terms

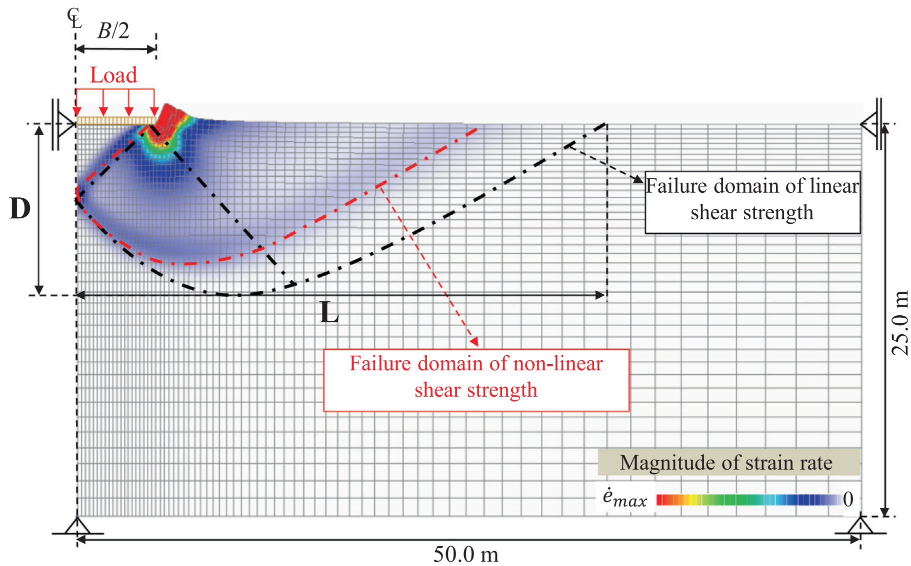

Fig. 7. Ground failure domains in case of $\phi_0 = 35°$, $B = 10$ m, and $\gamma = 18$ kN/m^3.

of normalized dimensions as compared to the total stress condition. This phenomenon can be attributed to the difference in mean effective stress in both cases. On the contrary, the size of the failure modes remains nearly the same in the case of the linear shear strength since the effect of the stress level is not considered in the postulate. Such a variation in the size of the failure zone needs to be carefully considered, specifically in urban areas where structures lie in close vicinity to one another and the performance of one structure may affect that of another. Based on the numerical investigations, it is rationally deduced that the proposal of a modification coefficient is imperative for the frictional term of the UBC formula in both the AIJ and JRA guidelines to properly account for the effect of stress dependency.

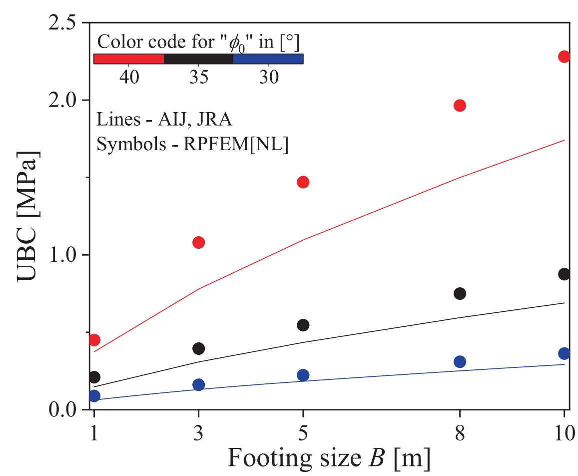

Fig. 8. Comparison of ultimate bearing capacity results in case of $\gamma = 8$ kN/m^3.

6. Ultimate bearing capacity formula for sandy soils

6.1. Modification coefficient for N_γ

An interesting finding in this study is that the combined effect of soil unit weight γ and footing size B governs the confining stresses in the soil. For instance, in the case of $\phi_0 = 35°$, the UBC of the footing size of 5 m at $\gamma = 18$ kN/m^3 is 948 kPa, while that of the footing size of 10 m at $\gamma = 9$ kN/m^3 is 949 kPa. As the mobilized shear strength in the soil remains the same for a constant value of the product (γB) of soil unit weight γ and footing size B, the UBC results also remain the same. This indicates that the size effect of the footing on the UBC is a function of the product γB. In this study, the term γB is normalized with respect to the atmospheric pressure, i.e., $p_a = 101.325$ kPa. In fact, De Beer (1965) initially introduced this concept and used ($\gamma B/\mathrm{E_q}$) to discuss the stress level effect through 1 g model tests, where $\mathrm{E_q}$ was the normalizing factor equal to atmospheric pressure p_a. Since then, this conceptualization has been used in centrifuge experimental studies (e.g., Zhu et al., 2001). The modification coefficient (η_γ) in the frictional term can be expressed as follows in the case of the centric vertical load (Eq. (11)):

$$\eta_\gamma = \frac{2q_u}{\gamma B N_\gamma} \tag{11}$$

The effect of stress term γB on modification coefficient η_γ is examined through bearing capacity analyses of the strip footing under the centric vertical load. The analysis results are arranged in Fig. 9 by numerically surveying the bearing capacity for the wide ranges in footing sizes of $B = 1$ m to 10 m, soil unit weights of $\gamma = 8$ kN/m^3 to 18 kN/m^3, and internal friction angles of $\phi_0 = 30°$, 35°, and 40°. The range in stress ($\gamma B/p_a$) considered in this study adeptly covers the range encountered in practical situations, i.e., 0.1–0.6 (Loukidis et al., 2011).

Table 4
Sizes of normalized failure domains in case of total and effective stress analyses.

ϕ_0 [°]	Footing B [m]	γ = 18 kN/m^3				γ = 8 kN/m^3			
		Non-linear		Linear		Non-linear		Linear	
		D/B	L/B	D/B	L/B	D/B	L/B	D/B	L/B
30	1	1.05	3.05	1.05	3.10	1.06	3.08	1.06	3.10
	5	0.84	2.29	0.93	2.74	0.92	2.51	0.94	2.75
	10	0.82	2.27	0.90	2.71	0.88	2.40	0.91	2.70
35	1	1.32	4.02	1.32	4.05	1.32	4.04	1.32	4.03
	5	1.05	3.00	1.18	3.60	1.12	3.28	1.19	3.63
	10	1.00	2.85	1.14	3.53	1.05	3.11	1.14	3.53
40	1	1.55	5.36	1.55	5.36	1.55	5.35	1.56	5.38
	5	1.26	4.20	1.41	4.91	1.33	4.55	1.43	4.91
	10	1.22	4.00	1.40	4.80	1.28	4.25	1.40	4.81

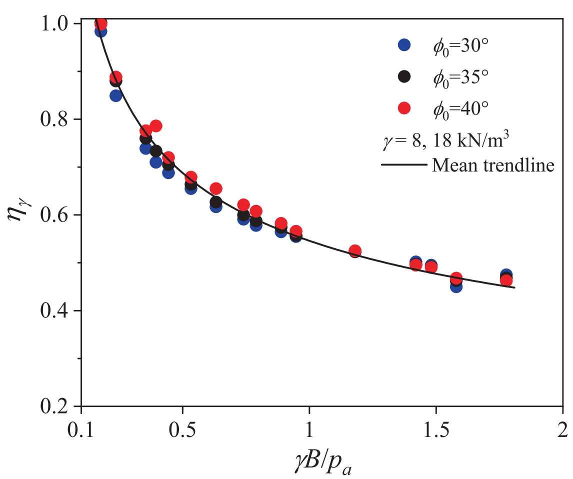

Fig. 9. Relationship between modification coefficient η_γ and $\gamma B/p_a$.

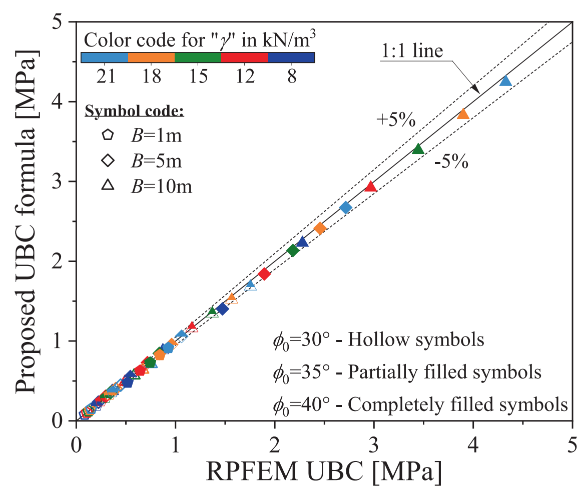

Fig. 10. Performance of proposed UBC formula against RPFEM analysis results.

The relationship between η_γ and $\gamma B/p_a$, based on the analysis conducted for the model sandy soil, is expressed by the mean trendline using the least squares method (Iqbal et al., 2022). The relationship for the mean trendline in Fig. 9 can be closely approximated by Eq. (12). The UBC formula for a strip footing on sandy soil, under the centric vertical load, is proposed as Eq. (13), in terms of the N_γ by Meyerhof (1963) and the modification coefficient (Eq. (12)). Meyerhof's bearing capacity factor N_γ is employed in the proposed equation (Eq. (13)) since the analysis results from the linear shear strength model, i.e., the RPFEM(DP), are consistent with those of Meyerhof. In addition, Meyerhof's bearing capacity factors are often referenced and recommended in foundation engineering manuals and guidelines (e.g., AIJ (1988, 2001, 2019)), and thus, widely used in engineering practice. In Fig. 10, the applicability of the approximated formula (Eq. (13)) is evaluated against the RPFEM analysis results through wide variations in soil properties and footing sizes.

$$\eta_\gamma = 0.55\left(\frac{\gamma B}{p_a}\right)^{\frac{-1}{3}} \quad 0 \leqslant \eta_\gamma \leqslant 1 \tag{12}$$

$$q_u = \frac{1}{2}\gamma B N_\gamma \eta_\gamma \tag{13}$$

6.2. Validation of proposed equation

The proposed UBC formula (Eq. (13)) is validated against the other prevailing UBC formulas, namely, AIJ, JRA, Eurocode, and USACE, for various analysis conditions, as shown in Fig. 11. In the case of γ = 18 kN/m^3, the proposed UBC formula shows a good match with the AIJ and JRA UBC formulas. However, in the case of γ = 8 kN/m^3, the AIJ and JRA formulas underestimate the UBC by nearly 20%. This is because both the AIJ and JRA formulas do not explicitly consider the stress level effect of γ on the size effect modification coefficient. On the other hand, the Eurocode and USACE UBC formulas overestimate the UBC as compared to the proposed UBC formula, AIJ, and JRA UBC formulas. This is primarily because neither the Eurocode nor the USACE formula adequately considers the effect of the confining pressure on the UBC rendered by the footing size and soil unit weight.

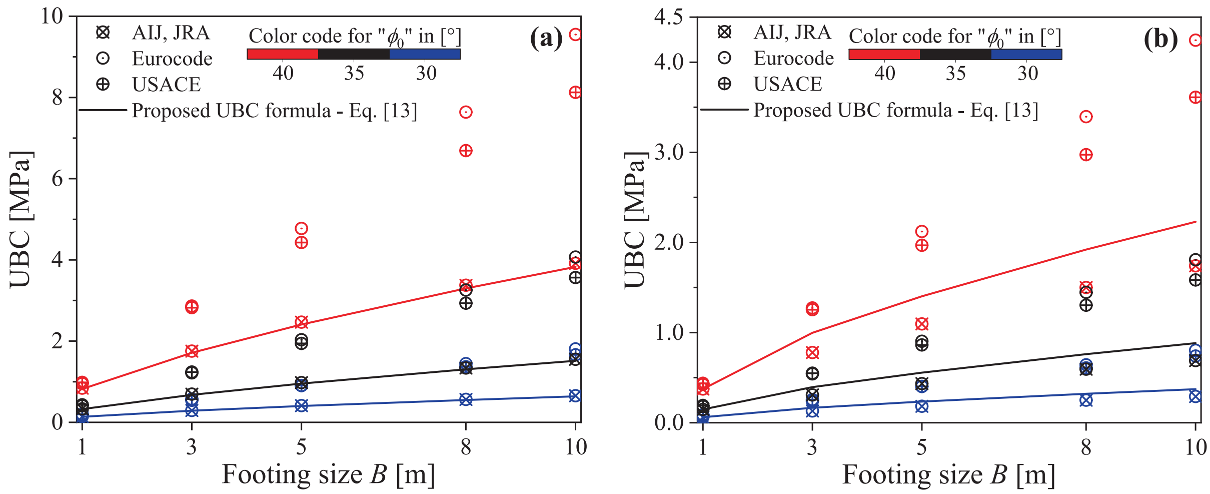

Fig. 11. Validation of proposed UBC formula: **(a)** γ = 18 kN/m^3 and **(b)** γ = 8 kN/m^3.

7. Discussion on ultimate bearing capacity formula for surcharge loading

7.1. Ultimate bearing capacity under surcharge loading

The well-known slip-line failure mechanism is depicted in Fig. 12, where I, II, and III represent the active wedge, radial shear zone, and passive Rankine zone, respectively, in the case of centric vertical load Q and uniform surcharge load q.

Pragmatically, footings are often subjected to surcharge loading q, as illustrated in Fig. 12. Nevertheless, bearing capacity studies that consider the effect of the stress level due to surcharge loading on the UBC still remain scarce, probably due to the intricacies associated with the preparation of the model setup. Amongst the UBC formulas/guidelines in Table 1, only the JRA specifications consider the modification coefficient in N_q. Therefore, it is pertinent to settle the discrepancies between the JRA guidelines and other UBC formulas/guidelines concerning the modification coefficient in the surcharge term of the equation. Furthermore, the JRA stress-dependent modification coefficients are proposed based on semi-experimental investigations for a limited range in surcharge ratios (q*=1–10), and hence, need to be validated through extensive numerical investigations. Moreover, the effect of multiple parameters, such as footing size, soil unit weight, internal friction angle, and surcharge, need to be thoroughly surveyed to correctly ascertain the factors governing the surcharge modification coefficient.

In this section, the non-linear shear strength parameters are used to analyze the UBC of a strip footing on model sandy soil under both centric vertical and uniform surcharge loads, i.e., 0 kPa to 90 kPa, for the same footing sizes and soil strength characteristics as in the previous chapters. The boundary conditions remain identical to those in the case of the centric vertical load only (Fig. 7). The RPFEM(NL) analysis results are plotted in Fig. 13 in comparison to those from the AIJ and JRA formulas to clearly illustrate the effect of non-linearity on the UBC with an increasing surcharge. The drop in the UBC through the RPFEM(NL) is mainly attributed to the effect of the variation in ϕ as the magnitude of confining stresses increases. Like conventional ultimate bearing capacity relationships, the AIJ formula considers the linearized effect of

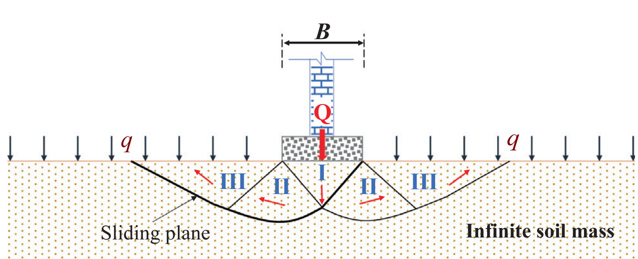

Fig. 12. General slip failure mechanism of footing B in sand under surcharge q.

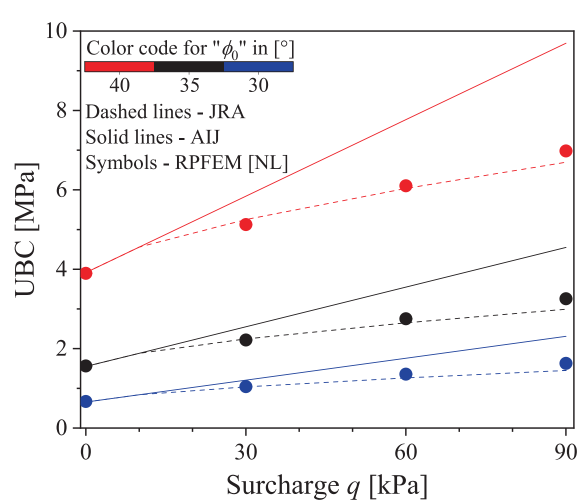

Fig. 13. Effect of surcharge load q on UBC in case of B = 10 m and γ = 18 kN/m^3.

the surcharge, thereby resulting in the substantial overestimation of the UBC (Fig. 13). However, the RPFEM(NL) analysis renders the ultimate bearing capacity as a non-linear function of the surcharge load, showing a good agreement with the JRA UBC formula in the case of γ = 18 kN/m^3 (Fig. 13). Therefore, in order to avoid the overvaluation in the UBC estimation under surcharge loading, it is essential to propose a surcharge modification coefficient to account for the effect of the stress level.

7.2. Modification coefficient for N_q

The RPFEM(NL) analyses results are utilized to propose the modification coefficient (η_q) in the surcharge term of the ultimate bearing capacity formula. The surcharge modification coefficient (η_q) is introduced as follows:

$$\eta_q = \frac{q_u - 0.5\gamma B N_\gamma \eta_\gamma}{q N_q} \tag{14}$$

The results are plotted in Fig. 14 to examine the general property of η_q against the footing size for the range in soil unit weights γ.

From the analysis results in Fig. 14, it can be observed that surcharge modification coefficient η_q remains nearly the same for the substantial variation in footing size B and soil unit weight γ. This demonstrates that the effects of the footing size and soil unit weight have already been well considered in frictional modification coefficient η_γ. Therefore, surcharge modification coefficient η_q is arranged against surcharge load q through normalization factor p_a (atmospheric pressure) in Fig. 15.

The mean trendline is drawn for the arranged dataset using the method of least squares (Fig. 15). The trendline adeptly represents the relationship between the surcharge load and the modification coefficient for a broad range of material parameters, footing sizes, and loading conditions. The relationship obtained from Fig. 15 takes the following form:

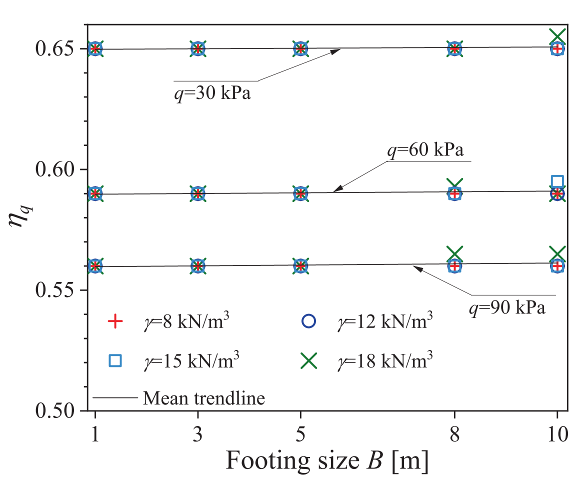

Fig. 14. General property of η_q against footing size B and soil unit weight γ in case of $\phi_0 = 35°$.

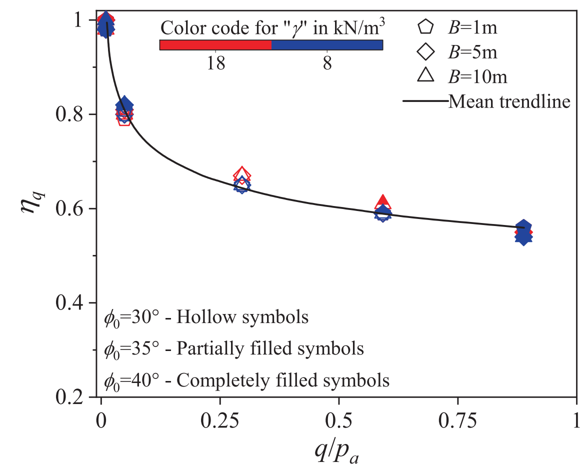

Fig. 15. Relationship between modification factor η_q and ($q_/ \ p_a$).

$$\eta_q = 0.55\left(\frac{q}{p_a}\right)^{\frac{-1}{8}} \quad 0 \leqslant \eta_q \leqslant 1 \tag{15}$$

Hence, the modified UBC formula can be written as Eq. (16) in terms of the bearing capacity factors, N_γ and N_q, proposed by Meyerhof (1963). Ohsaki (1962) carried out a series of bearing capacity experiments on ϕ and c-ϕ soils in order to estimate bearing capacity factors, N_c, N_γ, and N_q. Ohsaki (1962) recommended cutting off the bearing capacity factors at and beyond $\phi = 40°$, considering the fact that soils having an internal friction angle larger than 40° are not often encountered in practical circumstances and a small error in the laboratory measurement of the internal friction angle may cause the undue overestimation of the bearing capacity, particularly in the range beyond $\phi = 40°$. Likewise, the AIJ guidelines also recommend cutting off the bearing capacity factors at and beyond $\phi = 40°$. Therefore, this study also recommends cutting off the bearing capacity factors at and beyond $\phi = 40°$ to avoid any undue overestimation of the UBC for the reasons outlined above.

$$q_u = \left(\frac{1}{2}\gamma B N_\gamma \eta_\gamma\right) + \left(q N_q \eta_q\right) \tag{16}$$

Based on the results in this section, it is inferred that the conventional ultimate bearing capacity formulas, as well as the AIJ equation, lead to the overestimation of the surcharge load bearing capacity. In Fig. 16, the results obtained with Eq. (16) are compared to the results obtained with the UBC equation appearing in the JRA guidelines.

From Fig. 16, the proposed Eq. (16) estimates the UBC within ± 10% of the JRA formula in the case of γ = 18 kN/m^3. However, in the case of γ = 8 kN/m^3, the JRA formula underestimates the UBC by nearly 25%. This increase in difference is primarily because of the effect of soil unit weight γ on modification coefficient η_γ. The other guidelines, such as AIJ, Eurocode, and USACE, do not propose the modification coefficient in the surcharge term of the UBC formula, thereby resulting in the overestimation of

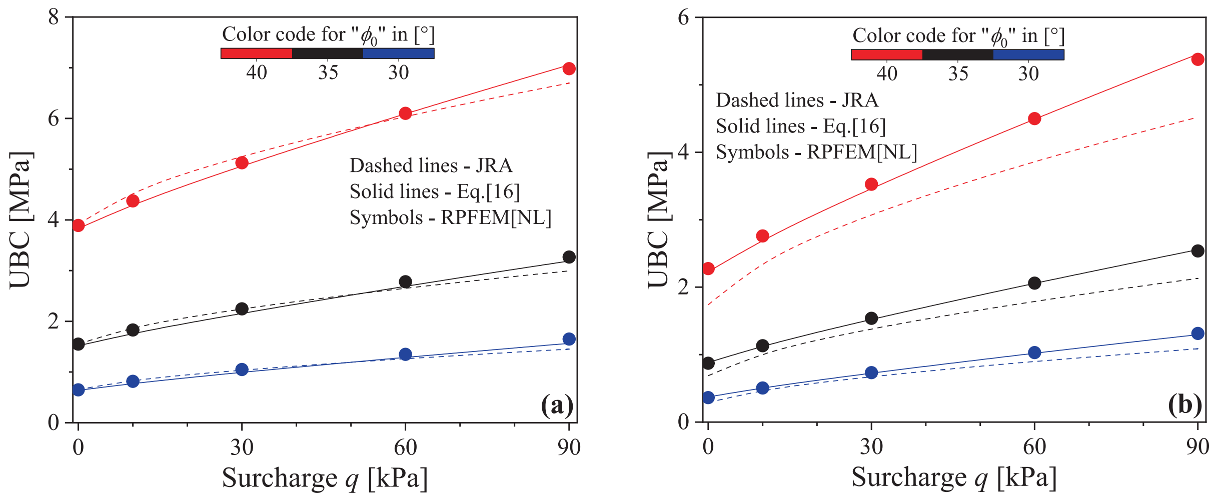

Fig. 16. Comparison of ultimate bearing capacity in case of B = 10 m: **(a)** γ = 18 kN/m^3 and **(b)** γ = 8 kN/m^3.

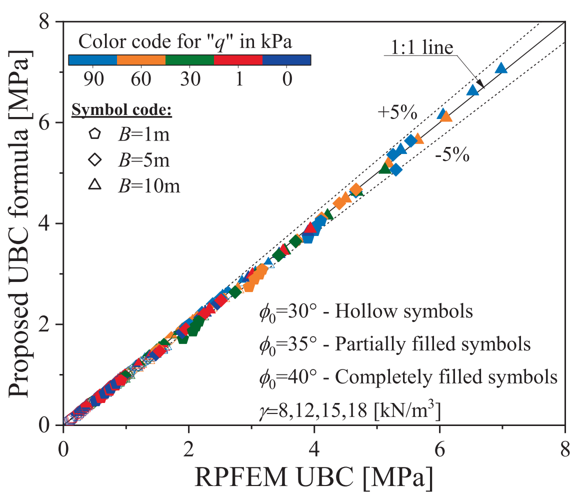

Fig. 17. Performance of proposed UBC formula against RPFEM analysis results.

the UBC. The proposed equation is better since it provides a good estimation of the UBC using a wide range of material characteristics based on the non-linear shear strength property. However, the JRA formula is overconservative and underestimates the UBC, whilst the AIJ formula overestimates the UBC under surcharge loading. Accordingly, the choice of the bearing capacity formula for the UBC estimation principally depends upon the assessment of the engineer in charge. Moreover, the performance of the proposed Eq. (16) has been randomly investigated for very heavy surcharges which were not used in the development of this equation. For instance, in the case of $\phi_0 = 35°$, $B = 30$ m, $\gamma = 18$ kN/m^3, and $q = 540$ kPa, the RPFEM analysis yields a UBC result of 11,231 kPa, while Eq. (16) yields a UBC result of 11,183 kPa, which is 99.6% of the analysis results. Therefore, it is corroborated that the proposed Eq. (16) accurately accounts for the effect of the footing size and the surcharge effect on the confining stress dependency of the shear strength parameters. As the proposed UBC formula (Eq. (16)) is approximated based on the analysis results, its performance is thoroughly examined against the RPFEM analysis results by widely varying the soil parameters, footing size, and surcharge load in Fig. 17.

8. Conclusions

The conventional UBC formulas (e.g., Meyerhof, 1963; Terzaghi, 1943) do not account for the effect of the stress level contributed by various parameters, namely, soil unit weight γ, footing size B, and surcharge load q. Therefore, this study has evaluated the UBC for broad ranges in footing sizes, material strength characteristics, and surcharge loads to properly ascertain the effect of the stress level through the non-linear shear strength property of Toyoura sand. Moreover, this study has provided a systematic survey of the UBC formula for various conditions of the soil properties and boundary conditions with the advantage of numerical analysis, which is otherwise difficult to examine through the model tests. The conclusions can be recapitulated as follows:

(1) The applicability of the RPFEM analysis to UBC estimations was proved to match the centrifuge experiments in the published references in the case of various sandy soils with lower to higher relative densities. A UBC formula was examined and improved based on the RPFEM analyses with the mechanical property of Toyoura sand in Japan. The failure domain of the ground became smaller due to the non-linear shear strength property in comparison with that from the Drucker-Prager strength model.
(2) The applicability of the modification coefficient for N_γ, in both the AIJ and the JRA guidelines, was found to be limited against the change in the soil unit weight. Through a numerical survey, the effect of the soil unit weight was clarified to be accurately indi-

cated by the normalized variable ($\gamma B/p_a$) in consideration of the size effect of the footing. Based on the numerical simulations, the modification coefficient for N_γ was newly proposed after past research on N_γ.

(3) The modification coefficient for N_q was not well investigated in the past, except in the JRA guidelines. However, it needs to be examined, considering the effect of the footing size and the soil unit weight. Moreover, the past guidelines did not explore the modification coefficient for N_q from the viewpoint of the various factors that affect the UBC. This study substantiated that the effect of the various factors on N_q is negligible; therefore, the modification coefficient for N_q depends only on the surcharge load. Finally, a modification coefficient for N_q was proposed based on the computed results. The aptness of the JRA specifications was discussed as being applicable from the engineering viewpoint.

(4) The performance of the proposed UBC formula was evaluated in comparison with the other formulas/guidelines and the RPFEM analysis in the case of wide ranges in footing size, soil unit weight, surcharge load, and strength parameters. The wide applicability of the proposed UBC formula was confirmed through its comparison with the RPFEM analysis case studies.

Acknowledgements

This work was supported by JSPS KAKENHI Grant Number JP18H01533. The authors greatly appreciate the financial support of Grant-in-Aid for Scientific Research (B) in Japan.

References

AASHTO, 2020. American Association of State Highway and Transportation Officials. LRFD Bridge Design Specifications (LRFDBDS-9), 9th edition, Washington, D.C. 20004, 1914p.

AIJ, 1988, 2001,2019. Architectural Institute of Japan. Recommendations for design of building foundations, 506p.

Asaoka, A., Ohtsuka, S., 1986. The analysis of failure of a normally consolidated clay foundation under embankment loading. Soils Found. 26 (2), 47–59.

Asaoka, A., Ohtsuka, S., 1987. Bearing capacity analysis of a normally consolidated clay foundation. Soils Found. 27 (3), 58–70.

Asaoka, A., Ohtsuka, S., Matsuo, M., 1990. Coupling analysis of limiting equilibrium state for normally consolidated and lightly overconsolidated soils. Soils Found. 30 (3), 109–123.

Clark, J.I., 1998. The settlement and ultimate bearing capacity of very large foundations on strong soils. Can. Geotech. J. 35 (1), 131–145.

De Beer, E.E., 1965. Bearing capacity and settlement of shallow foundations on sand. Symposium on Bearing Capacity and Settlement of Foundations, Duke Univ, Proc.

Eurocode, 2004. European committee for standardization. European standard for geotechnical design. Ref. No. EN 1997-1:2004.

FHWA, 2006. U.S. Federal Highway Administration. Soils and Foundations, Reference Manual-Volume-II, Publication No. FHWA NHI-06-089, Washington, D. C. 20590, 594p.

Hettler, A., Gudehus, G., 1988. Influence of the foundation width on the ultimate bearing capacity factor. Soils Found. 28 (4), 81–92.

Hijaj, M., Lyamin, A.V., Sloan, S.W., 2005. Numerical limit analysis solutions for the ultimate bearing capacity factor N_γ. Int. J. Solids Struct. 42, 1681–1704.

Hoshina, T., Ohtsuka, S., Isobe, K., 2011. Ultimate bearing capacity of ground by rigid plastic finite element method taking account of stress dependent non-linear strength property. J. Appl. Mech. 6, 191–200, in Japanese.

Iqbal, T., Ohtsuka, S., Isobe, K., Fukumoto, Y., Kaneda, K., 2022. Influence of footing size and relative density in ultimate bearing capacity formula of strip footing on sandy soils. In: 12th Int. Conf. on Geotechnique, Construction Materials & Environment, Bangkok, Thailand, pp.152-157 (in press).

JRA, 2017. Japan Road Association. Specifications for highway bridges part IV (substructures), 586p.

Loukidis, D., Salgado, R., 2011. Effect of relative density and stress level on the bearing capacity of footings on sand. Géotechnique 61 (2), 107–119.

Meyerhof, G.G., 1963. Some recent research on the bearing capacity of foundations. Can. Geotech. J. 1 (1), 16–26.

Nguyen, D.L., Ohtsuka, S., Hoshina, T., Isobe, K., 2016. Discussion on size effect of footing in ultimate bearing capacity using rigid plastic finite element method. Soils Found. 56 (1), 93–103.

Ohsaki, Y., 1962. Practical modification of bearing capacity factors in Terzaghi's formula. Proceedings of Architectural Institute of Japan 71, 35–40.

Okahara, M., Takagi, S., Obata, H., Mori, K., Tatsuta, M., 1988. Centrifuge tests on scale effect of bearing capacity. In: Proc. 42nd Japan Annual Conf. of Civil Engineers, Vol. III. pp. 250-251 (in Japanese).

Peck, R.B., Hanson, W.E., Thornburn, T.H., 1974. Foundation Engineering, 2nd ed. John Wiley and Sons, New York, NY, p. 544p.

Pham, Q.N., Ohtsuka, S., Isobe, K., Fukumoto, Y., 2019a. Group effect on ultimate lateral resistance of piles against uniform ground movement. Soils Found. 59 (1), 27–40.

Pham, Q.N., Ohtsuka, S., 2021. Ultimate bearing capacity of rigid footing on two-layered soils of sand-clay. Int. J. Geomech. 21 (7), 04021115.

Pham, Q.N., Ohtsuka, S., Isobe, K., Fukumoto, Y., Hoshina, T., 2019b. Ultimate bearing capacity of rigid footing under eccentric vertical load. Soils Found. 59 (6), 1980–1991.

Pham, Q.N., Ohtsuka, S., Isobe, K., Fukumoto, Y., 2020. Limit load space of rigid footing under eccentrically inclined load. Soils Found. 60 (4), 811–824.

Pham, Q.N., Ohtsuka, S., Isobe, K., Fukumoto, Y., 2022. Limit load space of rigid strip footing on cohesive-frictional soil subjected to eccentrically inclined loads. Comput. Geotech. 151 104956.

Poor, A.T., Barari, A., Behnia, M., Najafi, T., 2015. Determination of the ultimate limit states of shallow foundations using gene expression programming (GEP) approach. Soils Found. 55 (3), 650–659.

Prandtl, L., 1921. Über die Eindringungsfestigkeit(Härte) Plastischer Baustoffeund die Festigkeit von Schneiden. Z. Angew. Math. Mech. 1, 15–20.

Reissner, H., 1924. Zumerddruckproblem. In: Proceedings of the 1st International Congress of Applied Mechanics, Delft, The Netherlands, pp. 295–311.

Salgado, R., Bandini, P., Karim, A., 2000. Stiffness and strength of silty sand. J. Geotech. Geoenviron. Eng. 126 (5), 451–462.

Steenfelt, J.S., 1977. Scale effect on bearing capacity factor N_γ. In: Proceedings of the 9th International Conference on Soil Mechanics and Foundation Engineering, Tokyo, 10–15 July 1977. Japanese Society of Soil Mechanics and Foundation Engineering, Tokyo, Japan. 1, 749–752.

Tamboura, H.H., Isobe, K., Ohtsuka, S., 2022. End bearing capacity of a single incompletely end-supported pile based on the rigid plastic finite element method with non-linear strength property against confining stress. Soils Found. 62 (4) 101182.

Tamura, T., Kobayashi, S., Sumi, T., 1987. Rigid Plastic Finite Element Method for Frictional Materials. Soils Found. 27 (3), 1–12.
Tatsuoka, F., Goto, S., Sakamoto, M., 1986a. Effects of some factors on strength and deformation characteristics of sand at low pressures. Soils Found. 26 (4), 79–97.
Tatsuoka, F., Sakamoto, M., Kawamura, T., Fukushima, S., 1986b. Strength and deformation characteristics of sand in plane strain compression at extremely low pressures. Soils Found. 26 (1), 65–84.
Tatsuoka, F., Goto, S., Tanaka, T., Tani, K., Kimura, Y., 1997. Particle size effects on bearing capacity of footing on granular material. In: Asaoka, A., Adachi, T., Oka, F. (Eds.), Deformation and Progressive Failure in Geomechanics. Pergamon, pp. 133–138.
Terzaghi, K., 1943. Theoretical Soil Mechanics. John Wiley and Sons Ltd., p. 510.
Ueno, K., Miura, K., Maeda, Y., 1998. Prediction of ultimate bearing capacity of surface footings with regard to size effects. Soils Found. 38 (3), 165–178.
USACE, 1992. Department of the Army, U.S. Army Corps of Engineers, Bearing capacity of soils, Manual No. 1110-1-1905, Washington, D. C. 20314-1000, 196p.
Vesić, A.S., 1973. Analysis of ultimate loads of shallow foundations. J. Soil Mech. Found. Div. 99 (1), 45–76.
Vesić, A.S., 1975. Bearing Capacity of Shallow Foundations. Foundation Engineering Handbook. Van Nostrand Reinhold Company, New York, Chapter 3, 121–147.
Yoshida, T., Tatsuoka, F., 1997. Deformation property of shear band in sand subjected to plane strain compression and its relation to particle characteristics. Proc. 14th ICSMFE, Hamburg 1, 237–240.
Yoshida, T., Tatsuoka, F., Siddiquee, M.S.A., Kamegai, Y., 1995. Shear banding in sands observed in plane strain compression. In: Cambon (Ed.), Localization and Bifurcation Theory for Soils and Rock. Balkema, pp. 165–179.
Yoshimi, Y., Hatanaka, M., Oh-Oka, H., 1978. Undisturbed sampling of saturated sand by freezing. Soils Found. 18 (3), 59–73.
Zhu, F., Clark, J.I., Phillips, R., 2001. Scale effect of strip and circular footings resting on dense sand. J. Geotech. Geoenviron. Eng. 127 (7), 613–621.